UNIVERSITY OF Southampton

Interim technical report on the 2018 Surrey earthquake sequence

Dr. Stephen Hicks, 18/09/2018

Executive Summary

We have carried out analyses based on seismic data recorded from 15 earthquakes that occurred since 1 April 2018 in the south of Surrey, UK. The events occurred in the northern part of the Weald Basin, an area with little recorded and historically documented seismicity. The proximity of these events to nearby hydrocarbon exploration, development, and production activities means that this sequence has attracted a lot of public and media attention, making it important to make a robust characterisation of the seismicity. We base our analysis on seismic data from all available seismometers in the region, including the temporary local stations installed by the BGS Seismology team, and nearby stations part of the RaspberryShake citizen seismology network.

Using all available data, we find an additional two small events not in the BGS catalogue, and we can rule out any other events occurring before 1 April 2018. The earthquake starts like a typical mainshock-aftershock sequence on 1 April with a magnitude 2.6 event, but larger events in July means that this earthquake sequence shows characteristics of swarm-like behaviour. We re-pick and relocate the events using a region-specific velocity model constrained by sonic log information at nearby boreholes.

The epicentres of the earthquakes cluster to within ~6 km distance, centred on an area between the villages of Newdigate and Charlwood. There is also a slight east-west trend in the epicentral locations that correlate with the surface projection of a mapped normal fault within sedimentary rocks of the Upper Weald. Epicentral locations are well constrained even before the temporary local stations were installed in July 2018, but depths are poorly resolved. Better-constrained hypocentral locations from events on 2018-07-18 appear to show that these occurred at a shallow depth (< 900 m). The depth uncertainties on these events are low, but the station coverage is not perfect for resolving such shallow depths. An additional complication in our interpretation of these depths is the depth of a small (M_L 0.0) event on 2018-08-18, which has a well-constrained depth, and appears to have occurred at a somewhat greater depth of ~2.5 km.

In order to independently estimate event depths, we invert for the centroid moment tensors (CMTs) of events on 2018-07-18, which reveal information about the faulting mechanisms and are sensitive to source position. In a first step, we use low frequencies to negate the effect of unmodelled velocity heterogeneity in the subsurface; we find shallow centroid depths for these two events (300 – 800m), with a normal faulting mechanism. However, inversion of higher frequencies, which may be more sensitive to depth but more affected by subsurface structure, using a probabilistic Bayesian approach shows strike-slip faulting at ~1.7 km depth. Based on first-motion polarities, our preferred faulting mechanism is for left-lateral strike-slip faulting, with a small component of normal slip, along an east-west trending fault plane.

Overall, it is unclear whether the nearby industrial activities at the Brockham and Horse Hill sites induced the Surrey earthquakes. There is no clear precedence for this type of situation, with similar characteristics of the 2018 Surrey seismic sequence, globally with few similar case studies that were induced earthquake reported in the scientific literature. Furthermore, the physical mechanisms of fluid transfer and stress triggering in shallow sedimentary rock are poorly understood. We recommend that the temporary local seismic monitoring stations remain in place for the foreseeable future, and should there be any future earthquakes (or lack of earthquakes), any spatial-temporal correlation may be easier to rule in or out.

Email: s.hicks@soton.ac.uk
Direct tel: +44 (0)23 8059 9239

Disclaimer
Dr. Stephen Hicks' Post-doctoral position at the University of Southampton is funded by a NERC large grant (ref.: NE/K010824/1) on a project unrelated to this study. He receives no funding from any company or organisation related to the research in this document.

1. Introduction

We can expect many earthquakes in active tectonic regions, such as along plate boundaries of within distributed zones of highly-deforming plates. There is also potential for earthquakes within stable continental interiors, despite having low deformation rates. Earthquakes occur in these areas because background stress levels lie close to the strength limit of the crust. Therefore, under these critical conditions, small perturbations that affect fault stability can trigger earthquakes.

A “natural earthquake” is one for which failure occurs due to natural tectonic forces exceeding resisting frictional forces on pre-existing faults and for where is no evidence of anthropogenic influence . “Triggered earthquakes” are those that result from a small anthropogenic perturbation, causing a fault system to move from a near-unstable state to a fully unstable state. “Induced earthquakes” are those in which external anthropogenic activities cause failure within a rock that was not close to natural failure (Wilson et al., 2015).

Since 01 April 2018, the British Geological Survey (BGS) recorded sequence of 13 earthquakes were recorded in the south of the county of Surrey, UK, close to Gatwick Airport and the border with the county of Sussex. The largest of these earthquakes had a local magnitude (M_L) of 3.0.

The University of Southampton became involved in the project after discussing the installation of seismometers in the area with the BGS, and offering logistical support in the field. The BGS have shared continuous seismic waveform data from the new stations via an FTP site. Southampton's Geology and Geophysics group has a wide range of expertise in active and passive imaging of the Earth, analysing earthquakes at the local- and regional-scale along tectonic plate boundaries and active volcanic areas, and anthropogenic triggering of seismicity.

In recent years, seismicity induced and triggered by industrial operations has become an important topic of interest to the public, policymakers, and industry. The 2018 Surrey seismic sequence is a sensitive subject and has attracted significant public and media attention due in part to active hydrocarbon licence areas in the vicinity (within ~10 km); therefore, it is important to study these earthquakes and to assess whether any causal factors exist. However, attributing the cause of an earthquake to human activity, and discriminating between anthropogenic and natural seismicity is not trivial (Grigoli et al., 2017), when assessing short time periods of seismic and industrial data.

This report introduces the seismo-tectonic framework of the UK, then documents the data, the characteristics of the seismic sequence. Finally, we try to interpret characteristics of the sequence, comparing the sequence other similar seismic sequences around the world, both natural, and those that were induced.

2. Seismo-tectonic context

2.1. Causes of natural seismicity in the UK

The UK does not lie along an active plate boundary. Large faults dissecting the UK relate to ancient geological processes. Natural UK earthquake activity rarely impacts the public and infrastructure. Regional tectonic stress in the UK likely comes from "ridge push" forces in the Mid-Atlantic (e.g. Baptie, 2010), and northwest-southeast compression due to active collisional tectonics in the Mediterranean. Seismicity in the UK is not uniformly distributed (Figure 1). Some natural earthquakes across the British Isles can be associated with known fault zones, such as the Highland Boundary Fault Zone in Scotland (e.g. Ottemöller and Thomas, 2007).

2.2. Anthropogenic earthquakes

Besides natural earthquakes, the UK has experienced many anthropogenic earthquakes, most of which are caused by coal mining (e.g. Kusznir et al., 1980). For oil and gas extraction, most production in the UK occurs by conventional means. The 2001 M_w 4.3 Ekofisk earthquake in the North Sea was caused by stress changes due to water injection, rupturing the overburden at less than 3 km depth (e.g. Ottemöller et al., 2005). Furthermore, there is a spatial correlation between seismicity and oil and gas fields in the North Sea, suggesting a possible causal link (Wilson et al., 2015). In April 2011, the first UK multi-stage hydraulic fracturing of shale rock took place near Blackpool in Lancashire, which triggering an M_L 2.3 earthquake, located ~1.8 km from the Preese Hall 1 well, at 3.6 km depth (Clarke et al., 2014). 52 earthquakes with magnitudes ranging from between M_L 1.2 and M_L 2.3 occurred as part of this sequence. Classifying events in the UK seismic catalogue in the period 1970-2012, Wilson et al. (2015) suggest that ~21% of events in this period were caused by anthropogenic processes. Most past anthropogenic earthquakes in the UK are small (M_L<3.0) and occur at shallow depths (< 3 km).

2.3. South-east England and the Weald Basin

The Jurassic rocks of the Weald Basin in south-east England comprise an unconventional shale play (Wilson et al., 2015), with target reservoirs including the Kimmeridge Clay and Lower Oxford Clay (Andrews, 2014). The south-east of England is one of the least seismically active areas in the UK (Figure 1), with only five seismic events detected in the period 1970-2012. Surface and sub-surface mapped faults in the region trend east-west and show a normal sense of displacement. A wealth of 2-D seismic data from the UK Onshore Geophysical Library allows for a robust characterisation of pre-existing faults in the basin and depth-to-basement.

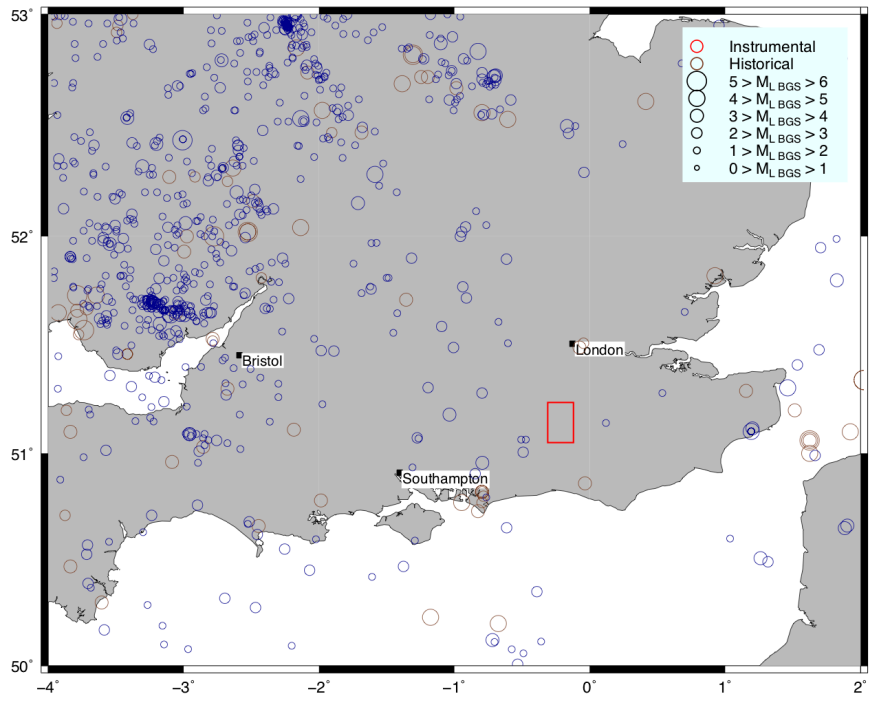

Figure 1: Past seismicity of the central and south-eastern regions of the British Isles from the instrumental and historical catalogues of the BGS. The red box shows the approximate area of the 2018 Surrey earthquake sequence.

3. Seismic stations

For our seismological analysis of the Surrey earthquakes, we include data from the following sources:

- Broadband stations of the BGS permanent backbone network up to ~200 km distance (stations: GB.CWF; GB.ELSH, GB.HMNX; GB.MCH1; GB.SWN1 GB.WACR).
- The borehole broadband station belonging to AWE Blacknest / Güralp Systems Ltd. in Wolverton, Hampshire (WOL).
- Short-period stations of the RaspberryShake citizen seismology project up to 70 km distance (AM.R034F; AM.R9621; AM.RAEBE; AM.RCC45; AM.REC60). Accurate locations of these stations come from the OSOP company, and they quote timing accuracy for these instruments as 10-20 ms[1]. Approximate timing and waveform polarities were cross-checked for consistency with permanent broadband stations through analysis of teleseismic earthquakes.
- Temporary broadband stations in the near-source area installed by BGS installed on 2018-07-12 (UR.HORS & UR.RUSH) and on 2018-08-13 (UR.BRDL; UR.GATW; UR.STAN).

The locations of these stations are shown in Figure 2.

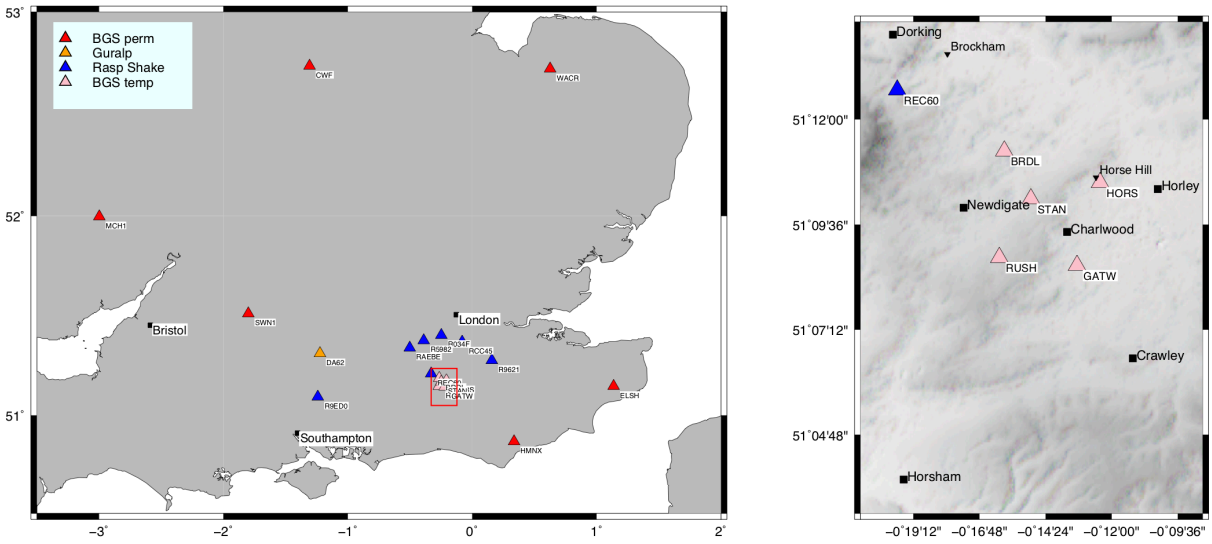

Figure 2: Maps showing the locations of seismic stations used in this study. The map on the right shows a zoom-in version of the area given by the red box in the map on the left.

[1] https://manual.raspberryshake.org/ntp.html

4. Event locations and magnitudes

4.1. Event catalogue

We first incorporated all thirteen events that recorded in the BGS catalogue from 2018-04-01 up to 2018-09-25.

To detect any additional events not in the BGS catalogue, we also ran a cross-correlation template matching algorithm on all local stations (AM.REC60, UR.HORS, UR.RUSH). For this, we used template waveforms incorporating P- and S-waves from the events in the catalogue. Using this approach, we detected two small additional events on 2018-04-09 and 2018-07-25. Our combined catalogue includes a total of 15 events.

For AM.REC60, we also scanned continuous waveforms before 2018-04-01, and going back as far as 2017-09-10 (when this station was first installed) to assess whether any small events had occurred before April 2018. We could not detect any earlier events; therefore, it is likely that the Surrey swarm started on, and not before, 1 April 2018.

The overall time/magnitude evolution of seismicity is shown in Figure 3.

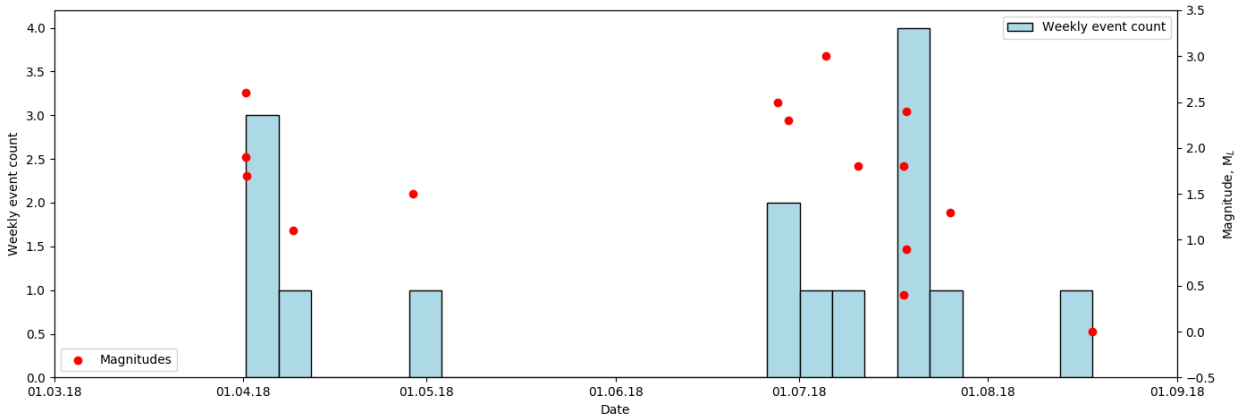

Figure 3: Time-magnitude evolution of the Surrey earthquake sequence, with event counts binned in weekly intervals.

4.2. Arrival time picks

We re-picked P- and S-wave arrival times from all events in the BGS catalogue, classifying the error on each pick due to arrival time uncertainty from 0 to 4 (where 0 shows the smallest error of ~0.1 s and 4 represents the largest error of > 1.5 s). Picking and initial relocation of events was performed iteratively, using the SDX software package[2].

4.3. Velocity model

A robust velocity model is needed for well-constrained earthquake locations, and to ensure there are no systematic errors in hypocentral locations. We assume a "minimum" 1-D velocity model that reflects the average velocity structure along each seismic ray-path, and should represent the near-source structure as accurately as possible. For event relocation, we based our 1-D seismic initial velocity model on constraints from the BGS's "General UK" model[3] and the CRUST1.0 model (Laske et al., 2013) for south-east England.

We then updated P-wave velocity model based on sonic logs from the Brockham (from the UK Onshore Geophysical Library) and Horse Hill wells (provided by UKOG). We tried different layer thicknesses and seismic velocity perturbations in terms of the stability of event locations, spatial clustering of events, and the average residual between observed and theoretical seismic wave arrival times. We also experimented with including a

[2] http://doree.esc.liv.ac.uk:8080/sdx/docs/SDX_manual.pdf

[3] http://earthwise.bgs.ac.uk/index.php/OR/18/015_Table_4:_Depth/crustal_velocity_models_used_in_earthquake_locations)

depth-varying S-wave velocity model based on Poisson's ratio constraints at the nearby Balcombe Well (provided by UKOG) and CRUST1.0. Overall, we found that a depth-varying shear-wave velocity resulted in longer arrival time residuals, so we used a constant Vp/Vs of 1.73, as per the BGS operational model, and is a robust global average value for continental regions.

Our preferred 1-D layered velocity model is shown in Table 1 and illustrated in Figure 4.

4.4. Magnitudes

For each event, we computed event magnitudes by computing the maximum zero-to-peak displacement in nanometres on 3-component waveforms in a window starting at the P-wave arrival, and ending at a time of 30 seconds plus the theoretical Lg arrival time (assuming a minimum Lg velocity of 3 km/s). Waveforms were low-pass filtered at 1.25 Hz, and we only used waveforms with a signal-to-noise ratio of greater than 2. Amplitudes were then used to calculate station magnitudes using the near-source scale of Butcher et al. (2017) for event-station distances of less than 17 km, and the scale of Ottemöller and Sergeant (2013) for all other stations. We then computed the overall event magnitude using a 25% trimmed mean to reject outliers.

Event magnitudes are illustrated in Figure 3 and shown in Table 2.

Depth to top of layer (km)	P-wave velocity (km/s)
0.00	2.60
1.20	3.10
1.50	3.60
1.80	4.70
2.10	5.00
2.10	5.00
2.40	5.50
7.60	6.40
18.90	7.00
34.20	8.00

Table 1: Our preferred 1-D P- layered velocity model used for event relocations, with a constant Vp/Vs ratio of 1.73.

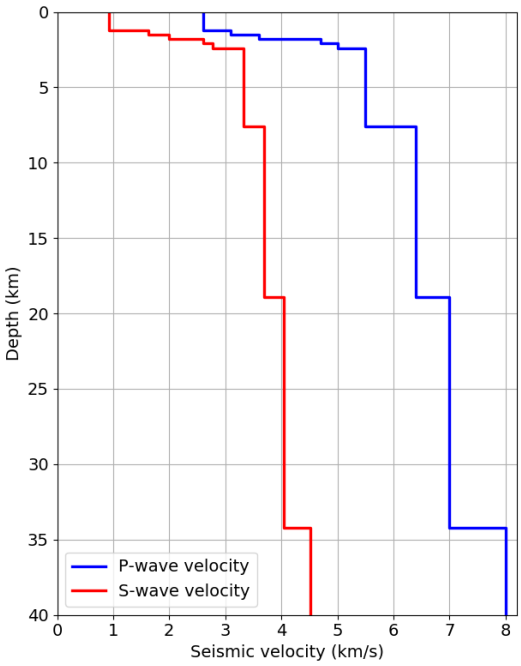

Figure 4: Our preferred 1-D P- and S-wave layered velocity model used for event relocations.

4.5.Single-event locations using NonLinLoc

To relocate the earthquakes, we used NonLinLoc (Lomax et al., 2009), which can provide more reliable and robust solutions compared with traditional single-event location codes. The equal differential time likelihood function implemented by NonLinLoc is very robust in the presence of outliers. It makes the automatic identification of false picks easier; they are discarded or down-weighted during calculations if an adequate number of total phases is present. The posterior probability density function (PDF) as computed by NonLinLoc represents a complete probabilistic solution to the earthquake location problem, including information on uncertainty and resolution.

The resulting locations from NonLinLoc are shown in Figure 5 and given in Table 2.

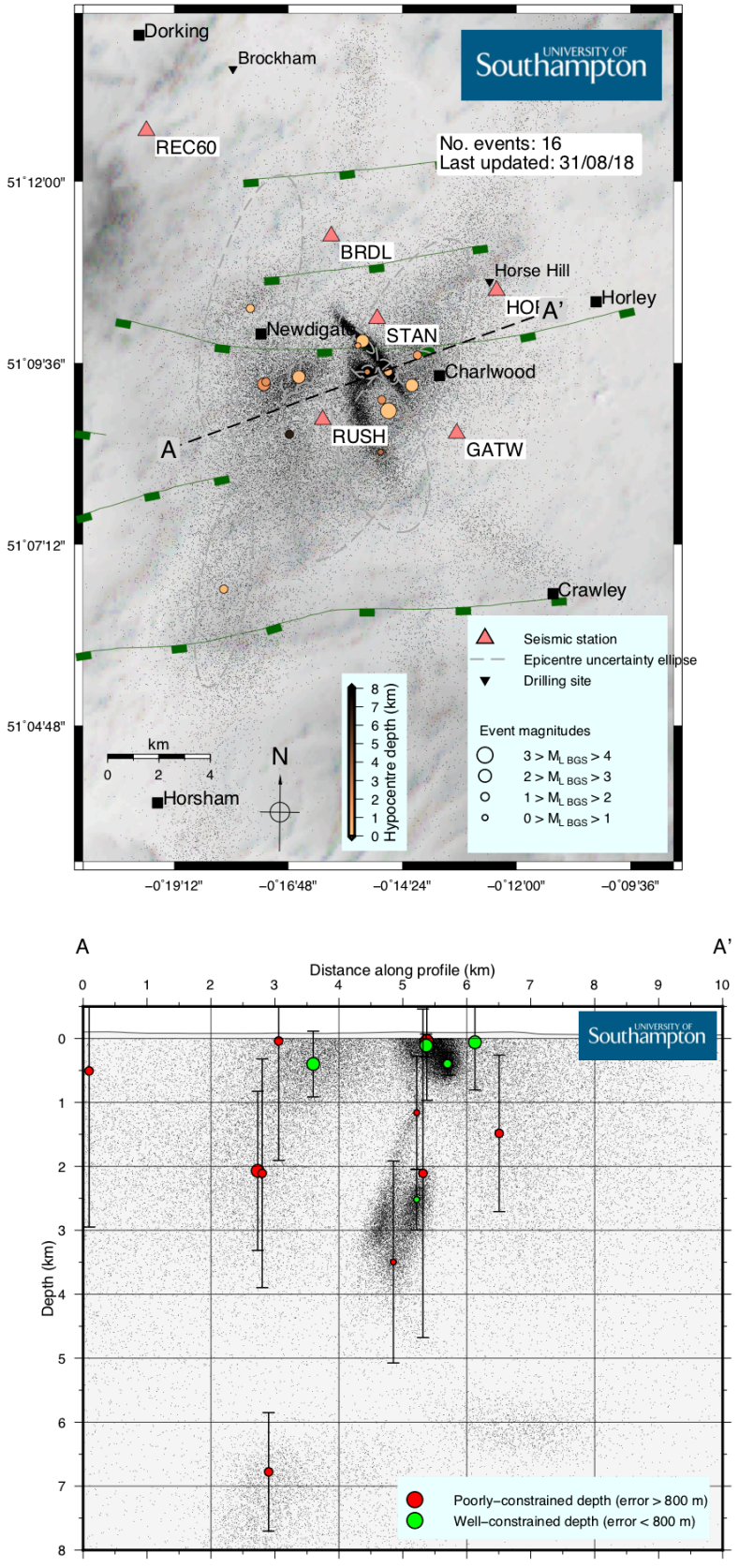

Figure 5: Map (top) and cross-section (below) showing the distribution of relocated seismicity using NonLinLoc. Location uncertainties are indicated by the grey error ellipses on the map and the depth error bars on the cross-section, as well as the gray density scatter points that illustrate the probabilistic location uncertainties. The surface projection of mapped subsurface faults from 2-D seismic reflection images are shown as green lines (James Verdon, personal communication).

Date	Origin time	Latitude (°)	Longitude (°)	Depth (km)	Latitude uncertainty (')	Longitude uncertainty (')	Depth uncertainty (km)	Magnitude (ML)	RMS residual (s)	Maximum azimuthal gap (')
2018-04-01	11:10:58.71	51.157	-0.276	0.40	0.0049	0.0051	0.51	2.6	0.31	158
2018-04-01	11:14:00.06	51.110	-0.303	0.51	0.0285	0.0085	2.44	1.9	0.45	169
2018-04-01	12:11:12.02	51.172	-0.293	0.04	0.0387	0.0152	1.87	1.7	0.5	157
2018-04-09	04:13:59.39	51.152	-0.247	2.11	0.0467	0.0259	2.57	1.1	0.65	169
2018-04-28	20:38:35.62	51.156	-0.288	2.11	0.0227	0.0103	1.79	1.5	0.6	159
2018-06-27	12:28:23.26	51.155	-0.237	0.06	0.0113	0.0076	0.75	2.5	0.43	137
2018-06-29	05:54:11.35	51.155	-0.289	2.07	0.0163	0.0079	1.24	2.3	0.66	139
2018-07-05	10:53:23.86	51.149	-0.245	0.04	0.0175	0.0146	0.93	3.0	0.53	138
2018-07-10	16:03:10.22	51.162	-0.235	1.48	0.0107	0.0078	1.22	1.8	0.48	135
2018-07-18	03:59:56.46	51.158	-0.245	0.40	0.0035	0.0029	0.18	1.8	0.29	106
2018-07-18	04:00:08.91	51.140	-0.248	3.50	0.0233	0.0142	1.58	0.4	0.1	255
2018-07-18	13:33:18.24	51.165	-0.254	0.11	0.0036	0.0033	0.18	2.4	0.25	79
2018-07-18	13:33:38.48	51.164	-0.256	1.16	0.0098	0.0057	0.89	0.9	0.05	137
2018-07-25	18:50:19.54	51.144	-0.280	6.78	0.015	0.0079	0.93	1.3	0.28	161
2018-08-18	03:21:58.16	51.158	-0.252	2.52	0.0019	0.002	0.47	0.0	0.04	96

Table 2: Location parameters from the NonLinLoc single-event relocation approach.

4.6.Multiple-event relocations using BayesLoc

To account for the variable station distribution with time, and the large uncertainties in event locations previous to the installation of RUSH & HORS, we carried out a multiple-event Bayesian relocation using the BayesLoc software package (Myers et al., 2007). Previous use cases have shown BayesLoc can significantly reduce the spread in hypocentre estimates (e.g. Gibbons and Kværna, 2017). Bayesloc finds a joint probability distribution for origins, hypocentres, and corrections to travel-time predictions. These Bayesian solutions typically result in more consistent time residuals over a given source region.

Locations and formal uncertainties from the NonLinLoc locations are used as priors in the Bayesian relocation. Therefore, the better constrained events have more stringent priors, ensuring that the locations of the most poorly constrained events are shifted the most.

The resulting locations from BayesLoc are shown in Figure 6.

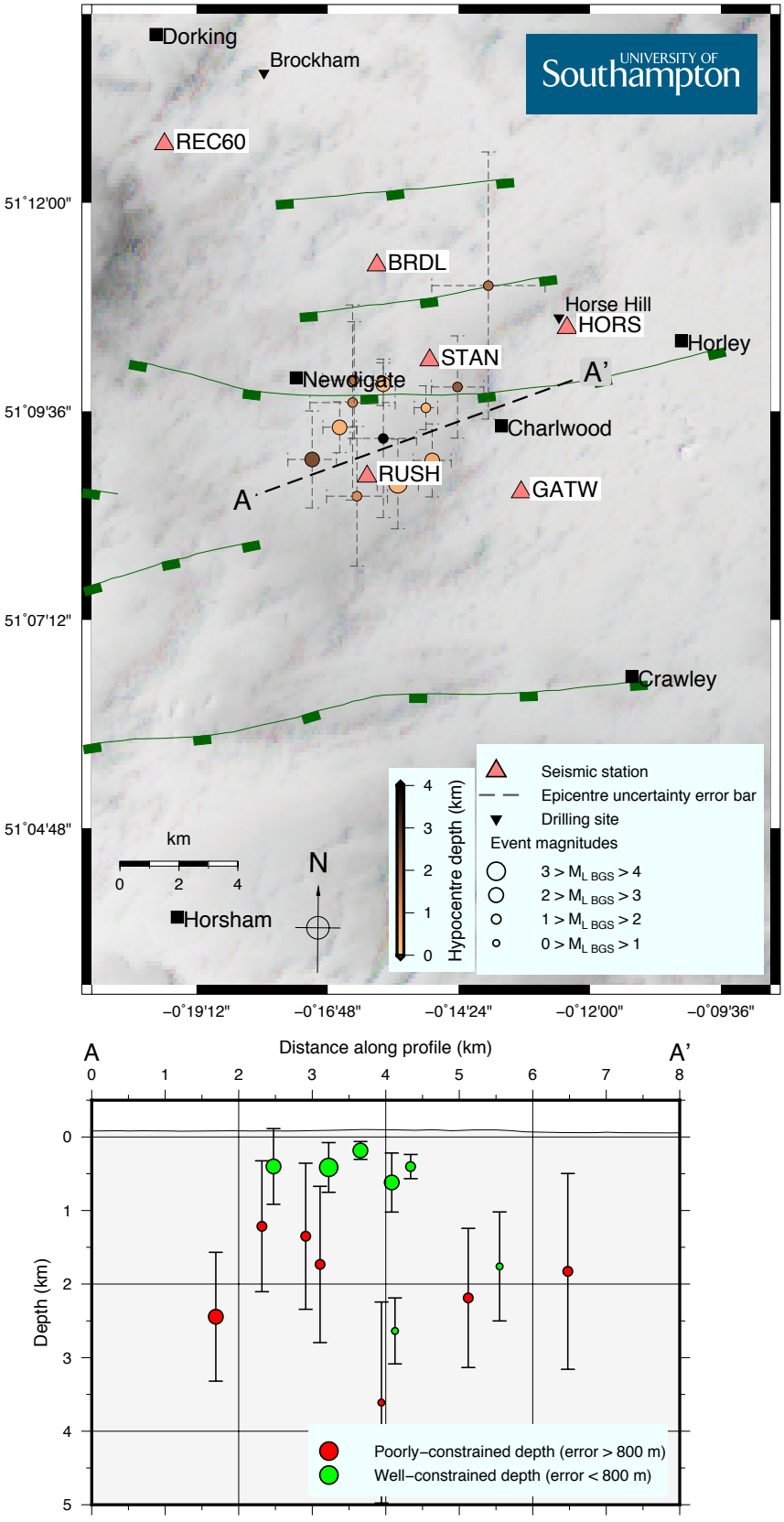

Figure 6: Map (top) and cross-section (below) showing the distribution of relocated seismicity using BayesLoc. Location uncertainties are indicated by the epicentral error bars on the map and the depth error bars on the cross-section. The surface projection of mapped subsurface faults from 2-D seismic reflection images are shown as green lines (James Verdon, personal communication).

5. Event mechanisms and depths from moment tensor inversion

Fortunately, the two temporary stations installed as part of the first phase were able to capture two of the larger events of the sequence on 18/07/2018, providing a unique opportunity to use full seismic waveforms to probe the rupture mechanisms, and to provide an independent constraint on source depth and timing.

Whilst using just two stations for moment tensor inversion is a sub-optimum situation, the availability of three-component waveform data at each station, with acceptable signal strength at long periods of ~50s to 10s and very strong signal at higher frequencies, provides a good chance for robust characterization of the seismic sources. Furthermore, past studies have showed that moment tensor inversion using data from sparse networks gives robust results (Dreger and Helmberger, 1991; Dreger et al., 1998; Dreger and Helmberger, 1993; Fan and Wallace, 1991; Ristau, 2008), especially if the following conditions are met: (1) the event-to-station distance is small to minimise any effect of noise on the waveforms; (2) the events to be studied are inside the network, and (3) the local velocity structure is well constrained.

Due to the critical influence of event depth on the interpretation of this seismic sequence, as well as the relatively large range in event depths given by the hypocentral relocations, we carry out source inversions using two independent methods.

5.1. Time-domain moment tensor inversion and grid-search for depth using low-frequency waveforms

For long-period waveform inversion, we use the ISOLA software (Sokos and Zahradnik, 2006), which uses a least-squares inversion to solve for moment tensor point-sources, with a grid search to solve for the best-fitting centroid time and position of point sources. We fix the centroid location at the hypocentre position, and allow centroid depth to vary with an interval of 200 m. Greens Functions were computed using the frequency-wavenumber algorithm of Bouchon (1981).

Waveform correlation as a function of depth and the observed-synthetic waveform fits are shown in Figure 7.

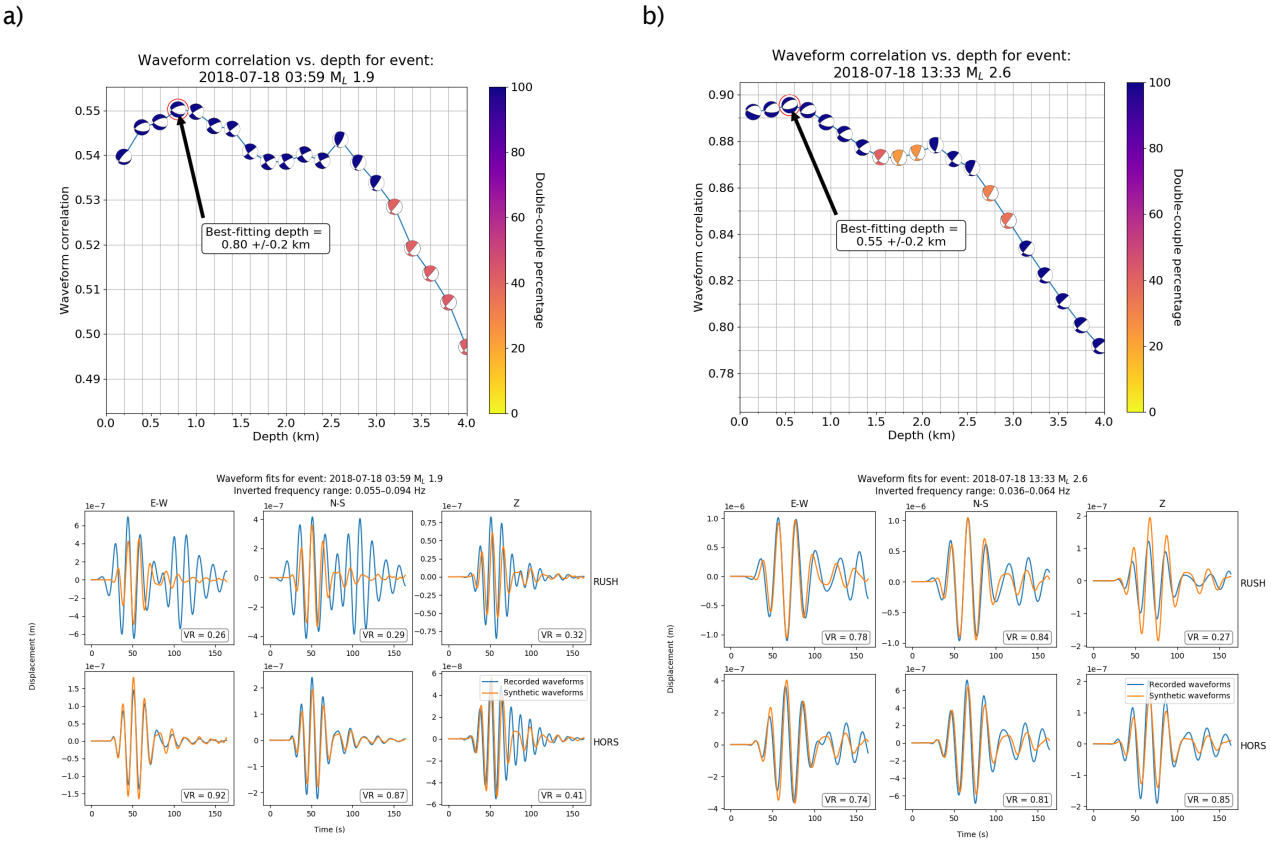

Figure 7: Waveform correlation (top) and synthetic-observed comparison (bottom) plots for the M$_L$ 1.9 (a) and M$_L$ 2.6 (b) events on 2018-07-18 using moment tensor inversion at low frequencies.

For both events, the results of the long-period moment tensor inversion show a stable solution of normal faulting along a west-east striking fault plane at a depth of 500-800 m depth.

5.2. Non-linear exploration of solution space using Bayesian bootstrap optimisation from high-frequency waveforms

5.2.1. Inversion method

To probe higher frequencies, and to explore the moment tensor solution space in a more probabilistic sense, we use the software Grond (e.g. Dahm et al., 2018), which part of the Pyrocko[4] open-source package for seismic analysis. Grond provides a framework to search model spaces in non-linear inversion problems. The default optimiser in Grond is a global Monte Carlo sampler, capable of retrieving multimodal and irregularly shaped solution spaces. It is a multi-objective function optimiser and can efficiently apply Bayesian bootstrapping to estimate earthquake source model uncertainties. It implements an efficient bootstrap-based method to retrieve solution sub-spaces, parameter trade-offs, and uncertainties in earthquake source parameter estimation problems.

In our case, we considered displacement waveforms of P and S phases filtered between 0.5 and 1.2 Hz for comparison with synthetic waveforms. Synthetic waveforms are modelled based on pre- calculated Green's functions assuming the minimum 1-D velocity model presented in Section 4.3. The Green's functions (GF) were calculated with the orthonormal propagator method using the program QSEIS[5] (Wang, 1999), for a 100 m grid spacing from 100 m to 10 km source-receiver distance, and between 100 m and 10 km source depth at a sampling rate of 8 Hz. We use a nearest-neighbour interpolation in between the grid points of the pre-computed Greens Functions.

Observed and synthetic ground displacement time series are filtered and windowed between from 2.5 s before the theoretical P-wave arrival time to 5.5 s after the theoretical S-wave arrival. The optimal time shift for alignment between processed observed and synthetic waveforms are determined by a grid search for each trial point source. We constrain the maximum time shift to be <0.5 s and a penalty misfit is added when shifting.

Deviatoric moment tensors, centroid times and coordinates are estimated through an optimisation algorithm. The source duration is not retrieved since we filter the data below the corner frequency of the earthquake; thus, our source model has nine degrees of freedom. We use 11 inversion parameters because we parameterise the moment tensor using its moment magnitude and six relative moment tensor entries and impose the deviatoric constraint during candidate source model generation. In every step of the optimisation, a new candidate source model is drawn from a dynamically updated search space distribution and evaluated in every of the perturbed objective functions.

5.2.2. Results

The best solutions for the two earthquakes on 2018-07-18 are shown in Figure 8 and Figure 9. The solutions were tested using slightly different frequency ranges, and are overall stable.

Both centroid depths are at ~1.7 km. Both events display a large double-couple component and represent a left-lateral strike-slip mechanism. Both events have similar nodal planes and the shifted centroid positions of both events are very similar (Figure 10).

[4] https://pyrocko.org

[5] https://github.com/pyrocko/fomosto-qseis

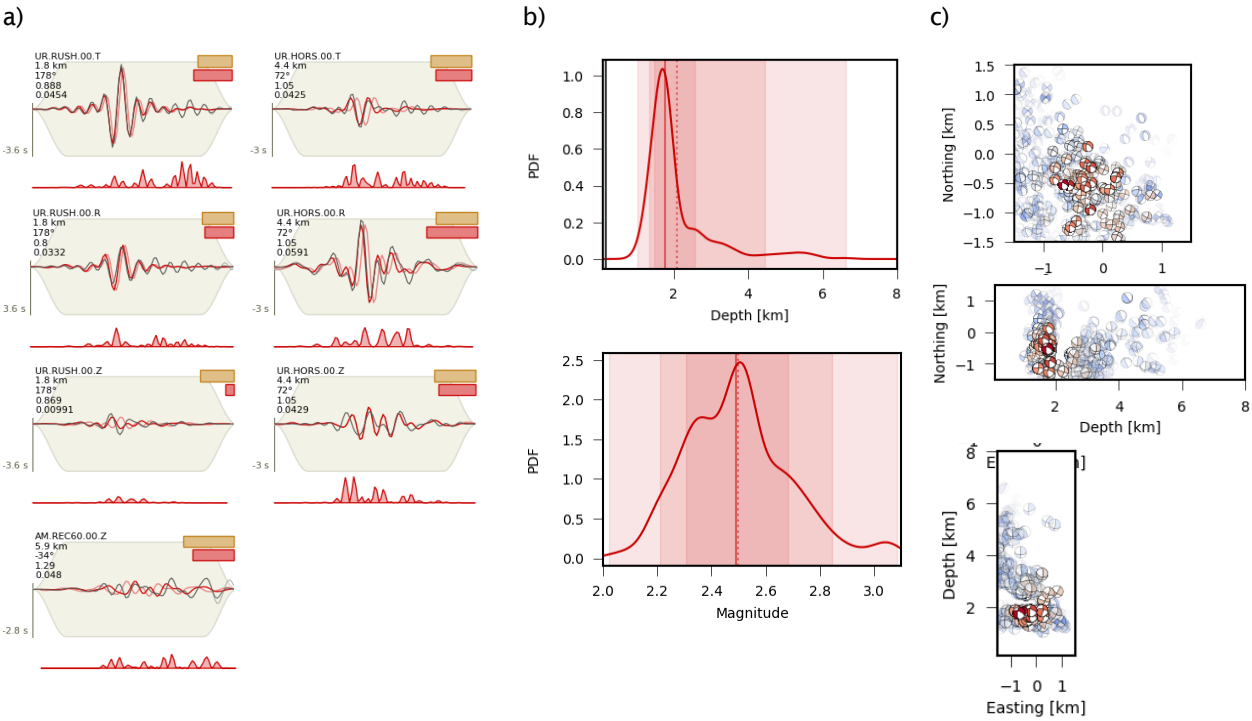

Figure 8: High frequency probabilistic moment tensor results for the ML 2.4 earthquake on 2018-07-18T13:33:18. a) Waveform comparison on the transverse (T), radial (R), and vertical (Z) components between observed (black) and synthetics (dark red) for the best-fitting solution. Light red waveforms are non-time shifted. b) Probability density functions for centroid depth and moment magnitude. c) Spatial clustering of centroid positions, with the red focal mechanism indicating the best-fitting solutions.

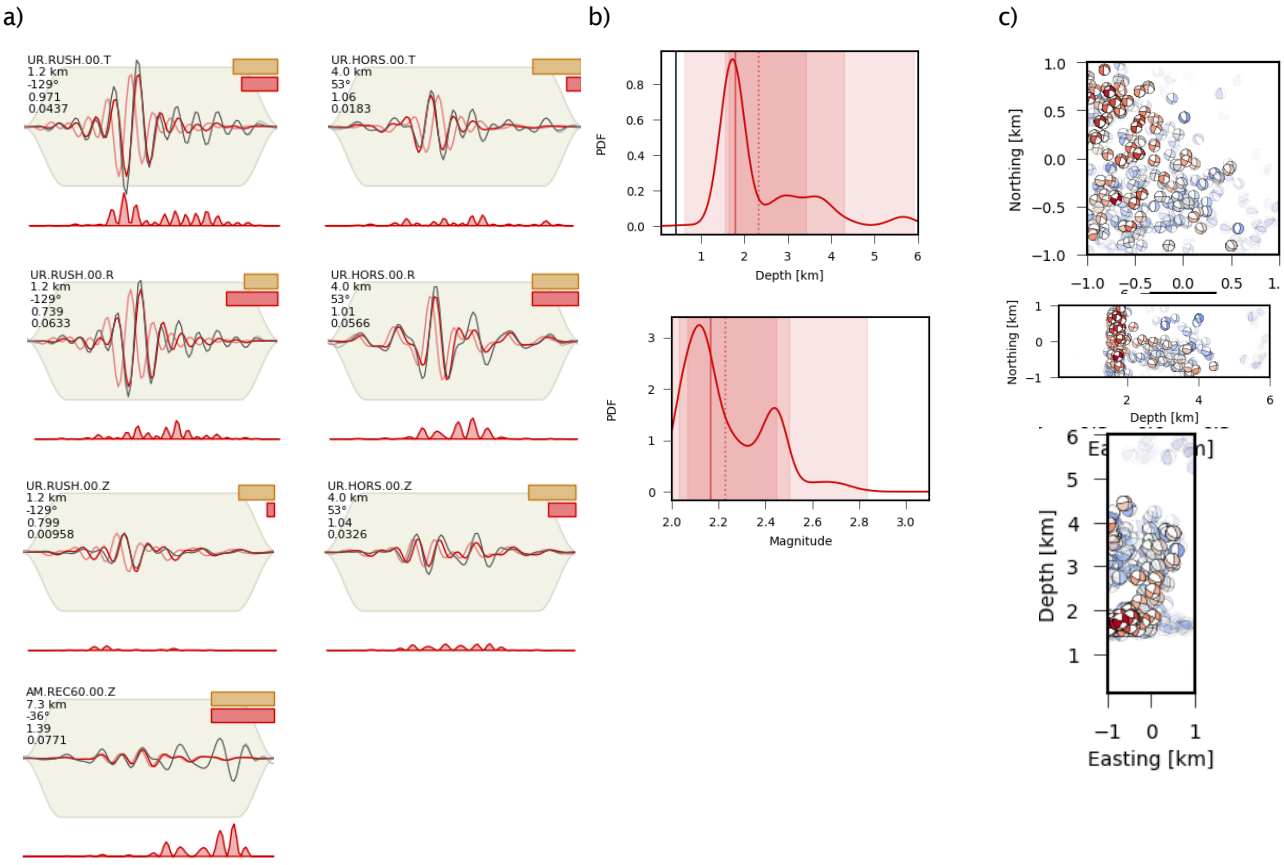

Figure 9: High frequency probabilistic moment tensor results for the ML 2.4 earthquake on 2018-07-18T03:59:57. a) Waveform comparison on the transverse (T), radial (R), and vertical (Z) components between observed (black) and synthetics (dark red) for the best-fitting solution. Light red waveforms are non-time shifted. b) Probability density functions for centroid depth and moment magnitude. c) Spatial clustering of centroid positions, with the red focal mechanism indicating the best-fitting solutions.

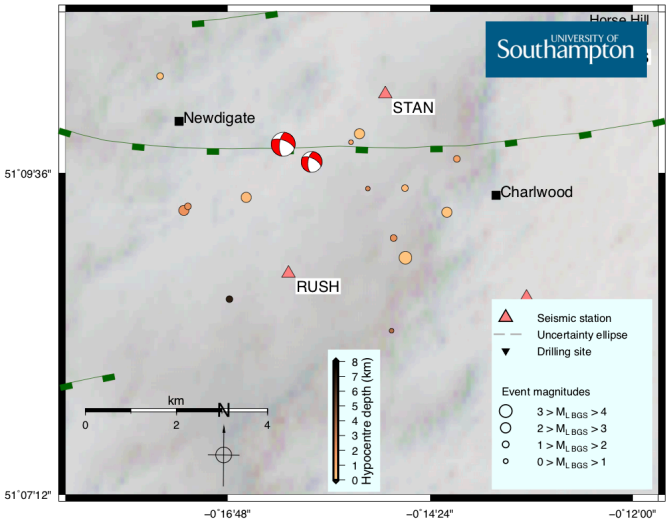

Figure 10: Map showing the NonLinLoc event locations, together with the focal mechanisms and centroid locations of the two events on 2018-07-18.

6. Discussion

6.1. Spatial distribution of events

The epicentres of the earthquakes cluster relatively consistently to within ~6 km distance, centred on an area between the villages of Newdigate and Charlwood. There is also an apparently and slight east-west trend in the epicentral locations that correlate with the surface projection of a mapped east-west striking normal fault within sedimentary rocks of the Upper Weald (Figure 5; Figure 6). Epicentral locations are reasonably well constrained even prior to the installation of the temporary local stations in July 2018, but depths are poorly resolved

6.2.Depth uncertainties

Overall, the event hypocentres and centroid depths from moment tensor inversion indicate a very shallow source of earthquakes, from 200 m to 2.5 km depth. Resolving depths in more detail within this range is a more complex task, which we will now briefly discuss.

The probabilistic error uncertainties given by the NonLinLoc locations for the best located events of the sequence indicate that the shallow hypocentral depths of <700 m, particularly for the M_L 2.4 and M_L 1.8 events on 2018-07-18, are reasonably robust given the realistic errors of the NonLinLoc algorithm (Figure 11). However, there is an apparent discrepancy with the hypocentral depth of the M_L 0.0 event on 2018-08-18, which has a calculated hypocentre depth of 2.5 km (+/- 500 m), and was well-recorded by all five near-field temporary stations. Given that the waveforms from the 2018-07-18 events and 2018-08-18 event are similar on the station UR.RUSH, one explanation is that all these events occurred at around the same depth. The difference between S- and P-wave arrival times at stations located small distances from events are typically used to constrain the depth of the earthquakes. However, using our optimal velocity model, we calculated that the difference between theoretical S-P times for a 2.5 km vs. 0.7 km source depth is only ~0.2 s for an event-station epicentral distance of 1.5 km (Figure 12). This short time difference may well be within typical picking errors and the exact pick times might be dependent on the exact waveform filter applied, particularly when considering the expected effect of event size on frequency content for M_L 2.4 and M_L 0.0 events.

Furthermore, one rule in depth sensitivity is that the closest stations (ideally three) should be within two times the expected depth of the earthquakes to resolve their depths. Therefore, with average station-event distances for the 2018-07-18 earthquakes (UR.RUSH and UR.HORS, which is less than the optimal three stations) being 2.8 km, we may not be able to resolve event depths of less than 1.4 km.

Shallow depths of < 1 km are consistent with the low-frequency moment tensor results show centroid depths of ~450 m and ~750 m, respectively, for the two events on 2018-07-18. However, higher frequency inversions for these events show a centroid depth of ~1.7 km.

Regardless of the exact depth of individual events of the Surrey earthquake sequence, there is overall substantial evidence that the earthquakes occurred within the Jurassic- to Cretaceous-aged sedimentary rocks of the Weald Basin (Figure 13). The strike of the possible focal mechanisms is consistent with these events occurring along a west-east fault; this type of fault is prevalent across the northern margin of the Weald Basin.

For comparison, if we take the BGS instrumental seismicity catalogue for the entire UK region, exclude events that occurred prior to 1990 (many of which was coal-mining related seismicity and have poorly constrained depths), exclude events with a fixed default depth of 5.0 km, and take events with M_L> 2.6, we find that events with depths of less than 2.5 km are reasonably uncommon (Figure).

6.3. Focal mechanism: normal faulting or strike-slip faulting?

The faulting mechanism given by the low frequency inversion indicates normal faulting; whereas the high frequency inversion indicates left-lateral strike-slip faulting (with a small component of normal faulting).

At a broad scale, the pattern of normal faulting indicated by the lower frequency moment tensor inversions, is relatively unusual in the context of the British Isles, with few large past events having this mechanism (Baptie, 2010). Normal faulting earthquakes may therefore represent a significant perturbation to the regional stress regime. However, the high frequency moment tensor result of left-lateral strike-slip faulting is more consistent with past seismicity on the UK mainland (Baptie, 2010).

Assuming that the mechanisms of the 2018-07-18 and 2018-08-18 events are the same, in spite of the difference in hypocentre depth, we can use observed first-motion polarities of these events to constrain the faulting mechanism. Figure 15 shows the observed polarities plotted onto the two possible focal mechanisms for the 2018-07-18T13:33 event. We find that there is a marginally better fit with the observed polarities for the high-frequency solution – strike slip faulting. In fact, the polarities that clearly do not fit this mechanism are from stations UR.STAN and UR.BRDL for the 2018-08-18 event. This discrepancy may indicate that the M

0.0 August earthquake may have a slightly different mechanism and/or depth uncertainty compared to the 2018-07-18 events.

As a result of the better fit, our preferred solution is for left-lateral strike slip faulting along a west-east fault plane with a small component of normal slip. Whilst the higher frequency inversion is likely to be favoured more by unmodelled seismic velocity heterogeneity in the subsurface, we favour the higher signal-to-noise ratio at higher frequencies, which ensures that possible noise sources are not contaminating the inversion results. Regardless of the sense of slip, a west-east trending fault plane is common to both mechanisms and correlates well with the local geological structure (Figure 5).

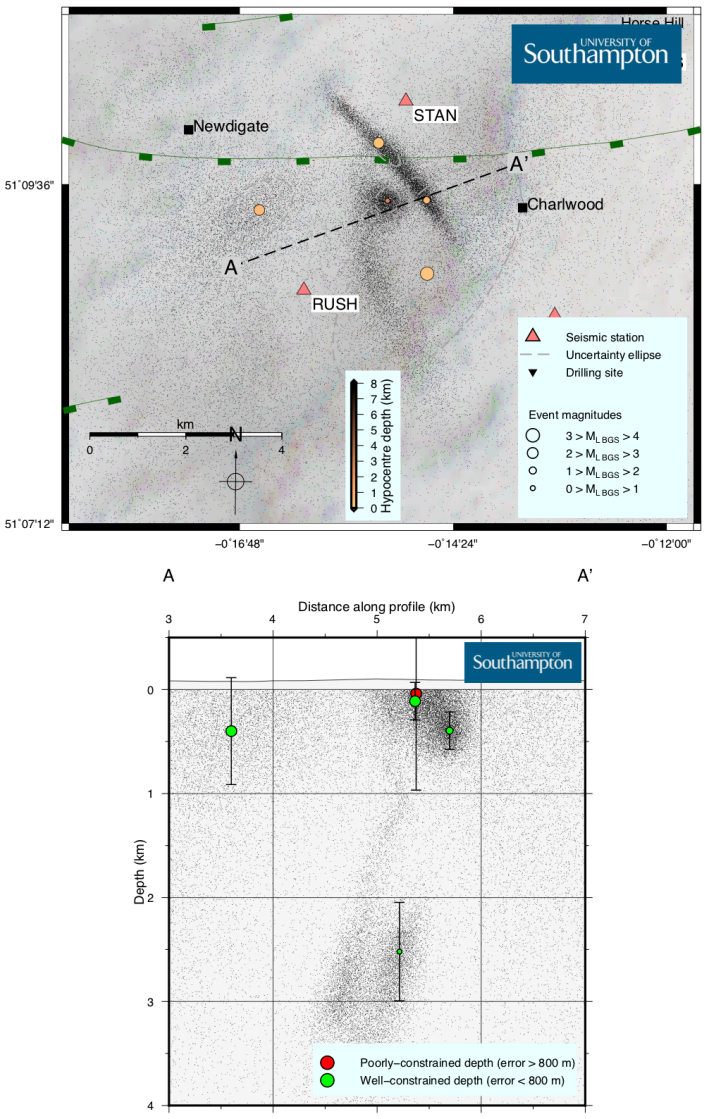

Figure 11: Zoomed-in version of the NonLinLoc locations plotted in map (top) and cross-section view (bottom) with probabilistic uncertainty scatter clouds for the best-constrained and/or largest five events of the sequence:

2018-04-01T11:10:58;

2018-07-05T10:53:23;

2018-07-18T03:59:56;

2018-07-18T13:33:18;

2018-08-18T03:21:58.

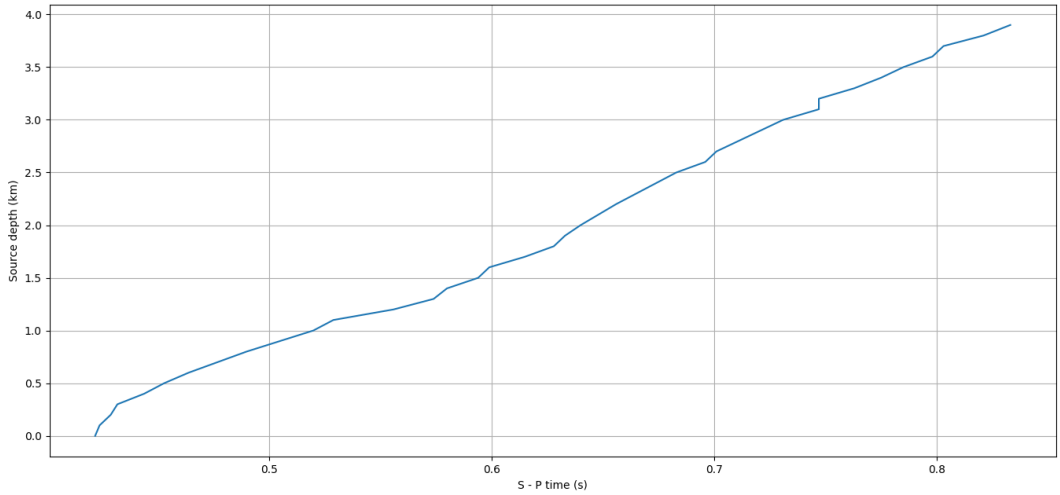

Figure 12: Theoretical S-P time vs. source depth for a source-station epicentral distance of 1.5 km.

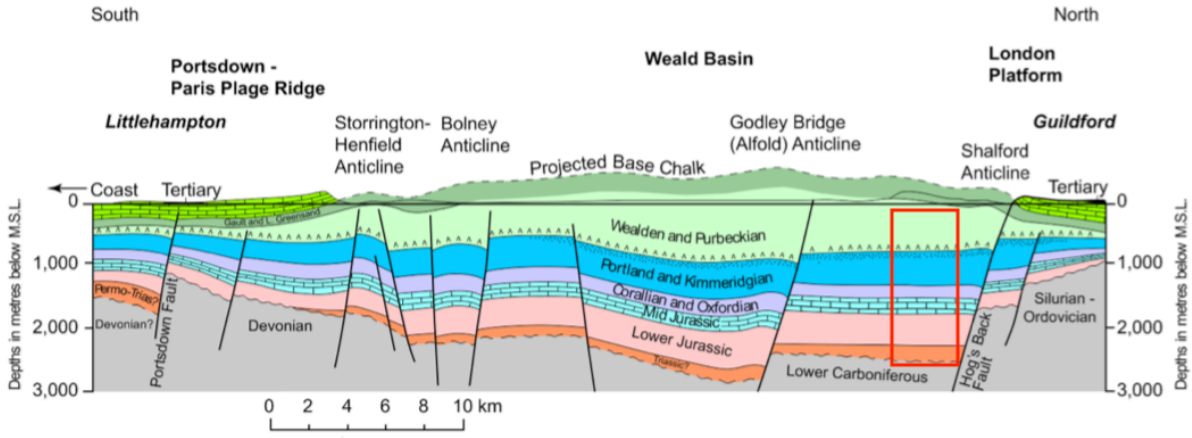

Figure 13: Schematic cross-section showing the subsurface geology of the Weald basin from south to north (after Butler and Pullan (1990)). The red box gives the approximate range in possible earthquake depths of the 2018 Surrey sequence.

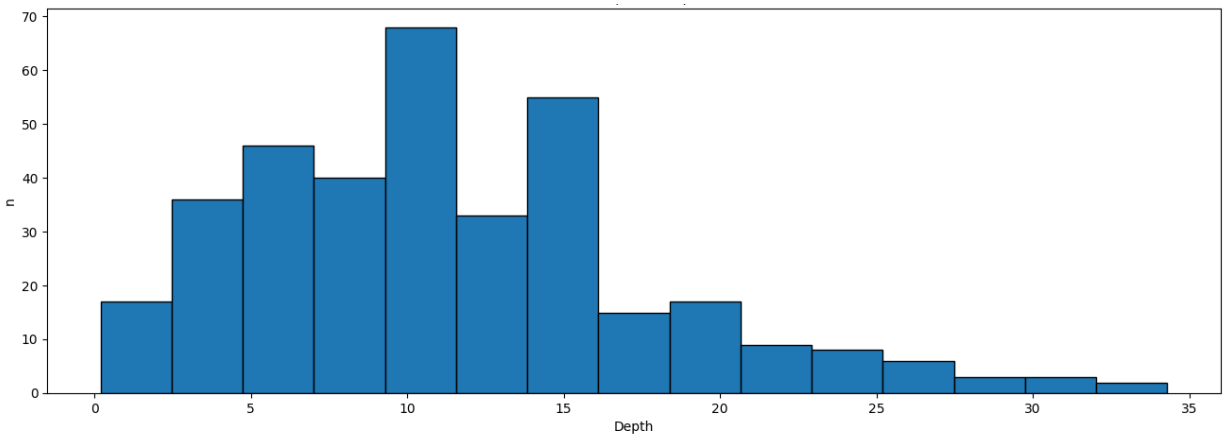

Figure 14: Histogram of event depths in the BGS instrumental seismicity catalogue for the British Isles from 1990 onwards. We have only considered events with M_L > 2.6 and excluded events with an apparent fixed default depth of 5.0 km.

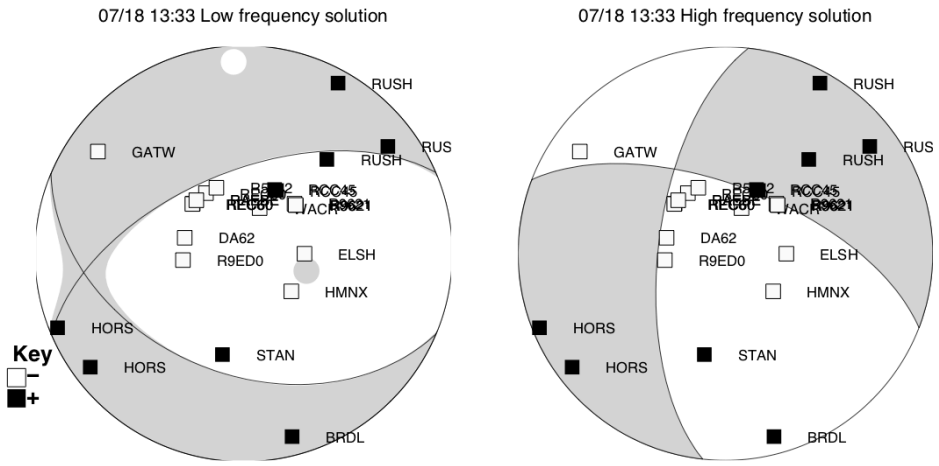

Figure 15: Possible focal mechanisms for the 2018-07-18T13:33 event, with projected first motion polarities from all events with the best-constrained locations in our catalogue.

6.4.Comparisons with case studies of past earthquakes sequences occurring at very shallow depths (< 2.5 km)

6.4.1. 2012 and 2015-2016 New Brunswick, Canada swarms

Bent et al. (2017) report on a set of seismic swarms in the New Brunswick region of eastern Canada in 2012 and 2015-2016. 28 events were recorded in 2012, and 22 events in 2015-2016. Three temporary seismographs were installed in the region due to the large number of felt events, which heightened public concern. The depth of these events was found to range from 0 to 1.2 km. These depths are consistent with the earthquakes occurring in Silurian meta-sediments, with a P-wave velocity indicating the crystalline nature of this rock. The authors were unable to explain the swarm activity and why it started suddenly in 2012, but human activity was ruled out as the underlying cause.

The swarm-like nature of this sequence and the very shallow depths draw parallels with the 2018 Surrey sequence. However, the major difference with the New Brunswick swarms is the type of geology inferred at the rupture depth of the earthquakes, with the Surrey events occurring in non-crystalline, clay-rich rocks, which are believed to have a low shear stress.

6.4.2. 2001 Ekofisk, North Sea earthquake

In May 2017, an Mw 4.1-4.4 earthquake occurred in the southern North Sea, which was felt strongly on platforms within the Ekofisk oil field (Ottemöller et al., 2005). Injection of water was used to reduce the long-term subsidence rate of the reservoir and overburden, with injection occurring at a rate of 700,000 barrels per day in 2005. The earthquake was found to have occurred at a very shallow depth of less than 3 km, indicating rupture of the overburden above the reservoir. The calculated focal mechanism of the earthquake indicates a normal-faulting sense of slip, with either slip on a near-horizontal plane or a near-vertical plane. Rupture was believed to occur due to increased pore pressure due to water injection into clay-rich shales, indicating that Mw>4 earthquakes can occur within over-pressure and poorly consolidated clay-rich rocks at shallow depth.

This Ekofisk earthquake is similar to the Surrey sequence in terms of the shallow depth of rupture in weakly-consolidated and low shear strength sediments and the possibility of normal faulting. However, the long-term extraction and injection at Ekofisk are expected to be on many orders of magnitude larger than those at the Brockham and Horse Hill wells.

6.4.3. 1997 & 2010 Alice, Texas earthquakes

Frohlich et al. (2012) reviewed a magnitude 3.9 earthquake that occurred in southern Texas in 2010, which had similar characteristics to an earthquakes in 1997. Both earthquakes occurred within 3 km of a major petroleum field, the Stratton field, with a reservoir comprising sand-rich deposits. The earthquakes occurred at shallow depths of 3 km or less. Considerable amounts of oil produced – 100 million barrels, with an aerial extend of 100 km^2. A tenuous temporal correlation – 25-40 years after peak withdrawal rates.

From this sequences, three possible mechanisms of shallow rupture were proposed:

- Increased pore pressure due to injection decreases normal stress, allowing fracture following the Coulomb criterion. (ML<3)
- Fluid withdrawal causes a change in pore pressure, which causes changes in the geological structure. Stress changes are transferred to the area immediately surrounding the reservoir. Believed to lead to reversed faulting (Segall. 1989).
- Massive load removal during hydrocarbon extraction – crustal adjustments to stress changes.

However, in contrast to the northern Weald area, the Stratton field has likely seen much higher volumes of hydrocarbon extraction, leading to a depleted reservoir and possible large-scale subsidence.

6.5.Qualitative discrimination between induced and natural seismicity

6.5.1. Davis and Frohlich (1993) criteria

Davis and Frohlich (1993) set out a list of seven questions with YES/NO criteria, considering several factors such as the spatiotemporal correlation between seismicity and industrial activity, or the change in the background seismicity rate. This set of criteria is mainly focussed on fluid injection activities. The relative number of YES / NO answers gives a coarse indication of whether events were induced by fluid injection.

1) Background seismicity. Are these events the first known earthquakes of this character in the region?

   ***Yes**. Aside from the 1551 earthquake reported in Dorking and Greater London areas, there is no evidence of earthquakes with magnitudes of greater than 2 km occurring the Surrey and Weald Basin area, especially in instrumental catalogues.*

2) Temporal correlation. *Is there a clear correlation between injection and seismicity?*

   ***Yes**, based on available evidence, there appears to be a strong temporal correlation with the commencement of production and injection activity at the Brockham Well in April 2018. Flow test operations occurred within two years of the start of the 2018 seismic sequence, although it is unclear whether this had the mechanism to induce earthquakes.*

3) Spatial correlation

   a) Are epicentres near wells (within 5 km)?

      ***Yes**. The epicentres are ~4 km from the HH-1 well, but > 7 km from the Brockham Well.*

   b) Do some earthquakes occur at or near injection depths?

      ***Yes**, there is evidence from hypocentre locations and moment tensor solutions that indicate shallow depths (< 2 km), which appear to correlate with depths of development and production targets in the Weald Basin (e.g. Portland Sandstone Fm.; Kimmeridge Shale formation), particularly at the Brockham Well, where fluid injection has occurred. It is unclear whether any injection of fluids have occurred at the HH-1 Well.*

   c) If not, are there any known geologic structures that may channel flow to sites of earthquakes?

      ***No(?).** Although high porosity and high permeability formations (comprising e.g. sandstone) may act as a fluid pathway, there is no evidence to suggest such fast channel flow between the commencement of operations at Brockham in April 2018 and the start of the earthquake sequence.*

4) Injection practices

   a) Are changes in fluid pressure at well bottoms sufficient to encourage seismicity?

      ***No(?).** Based on precedents in the scientific literature it seems unlikely that the flow testing operations at HH-1, and the amount of fluid removed and injected at Brockham were sufficient to have induced large-scale stress changes, although these threshold volumes and rates are poorly known and probably depend on local geological properties.*

   b) Are changes in fluid pressure at well bottoms sufficient to encourage seismicity?

      ***No(?).** See answer to 4)a).*

Overall, with four "Yes" answers and two "No" answers to these questions, there is some indication that the 2018 Surrey earthquakes were possibly induced.

6.5.2. Frohlich et al. (2016) criteria

More recently, Frohlich et al. (2016) updated their question-based approach which applies both to injection-induced events as well as those caused by other mechanisms, this time scoring the answers to classify seismicity into four groups: *tectonic*, *possibly induced*, *probably induced*, and *almost certainly induced*. These criteria are more suitable for discriminating induced seismicity in tectonically stable regions (Grigoli et al., 2017).

1. Timing: In this location, are earthquakes of this character known to begin only after the commencement of nearby petroleum production or fluid injection operations that could induce seismic activity?

   ***No**. There is no past precedent for similar earthquakes occurring around the UK that are known to have been induced by the types of petroleum production and injection activities occurring in Surrey.*

2. Spatial correlation: Are the epicentres spatially correlated with such production or injection operations (i.e., within 5 km for well-determined epicentres or within 15 km otherwise)?

   ***Possibly**. Although the epicentres are well-constrained laterally and within 5 km of the HH-1 well, based on available evidence, there is no evidence to suggest that the flow test operations at HH-1 could have induced the earthquakes. In addition, the well-located epicentres are > 7 km from the Brockham well, where production and injection activities were being carried out at the time of the Surrey earthquake sequence.*

3. Depth: Is information available concerning focal depths of earthquakes at this location, and does this suggest some depths are shallow, probably occurring at or near production or injection depths?

   ***Yes**, there is evidence from hypocentre locations and moment tensor solutions that indicate shallow depths (< 2.5 km), which appear to correlate with depths of development and production targets in the Weald Basin (e.g. Portland Sandstone Fm.; Kimmeridge Shale formation).*

4. Faulting: Near production or injection operations, are there mapped faults or linear groups of epicentres that appear to lie along a fault? Here, "near" is within 5 km if the earthquake or earthquake sequence of interest has well-determined epicentres, or within 15 km otherwise.

   ***Yes**, earthquakes of the 2018 Surrey sequence appear to spatially correlate with mapped faults to within 5 km.*

5. Published analysis: Is there a credible published paper or papers linking the seismicity to production or injection operations?

   ***No** - not currently, although a peer-reviewed paper is planned.*

Based on these answers, the total score is 2.5, which according to these criteria, indicate the earthquakes are **"probably induced"**.

6.6. Outstanding issues

Although the results of these qualitative criteria indicate "probable"/"possible" induced seismicity, there are still a number of uncertainties and these questioning schemes do not explain the physical mechanisms required for induced seismicity in different circumstances.

Based on our understanding of different cases of induced seismicity around the world, fluid injection and/or extraction processes at nearby sites does not appear to have been carried out at sufficiently large volumes and/or rates to have been a prime candidate for inducing seismicity. Furthermore, there is little precedent for conventional hydrocarbon extraction processes to have directly induced seismicity, particularly in non-depleted reservoirs.

Conversely, most research surrounding induced seismicity, particularly waste-water injection has focussed on stressing faults in the crystalline basement, and the response of shallow sediments to even small changes in induced fluid pressure is poorly known. Recently, Goebel and Brodsky (2018) showed that injecting fluid into sedimentary units may trigger larger earthquakes occurring at greater distances from the injection site

compared to injecting into crystalline rocks, due to efficient pressure and stress transmission. But, if this relationship does exist for the Surrey earthquakes, it does not explain the lack of recorded seismicity for the 4 - 8 km between the active cluster and the nearby wells.

If these seismic events are induced, we have not yet considered a possible time lag effect. Induced seismicity has shown to be delayed by up to months and years following a change in subsurface conditions (Ellsworth, 2013; Simpson et al., 1988). Therefore, any future investigation should consider the long-term production and injection activities at the Brockham Well, as well as the 2016 flow test at the Horse Hill well.

6.7. Further work and recommendations

The somewhat swarm-like nature of 2018 Surrey earthquake sequence is characterised by the relatively large number of events compared to the size of the largest event in the sequence (Holtkamp and Brudzinski, 2011; Vidale and Shearer, 2006). This swarm-like behaviour may be characteristic of an induced earthquake sequence (Skoumal et al., 2015). However, natural swarms have been known to occur around the British Isles, such as the 1974 Kintail, Scotland sequence (Assumpção, 1981), the 2002 Manchester sequence[6], and the 2003 Aberfoyle, Scotland swarm (Ottemöller and Thomas, 2007). Therefore, other key characteristics of the seismicity are needed to discriminate induced seismicity. For example, future work should try to constrain relative stress drop values of the largest events in the sequence because induced earthquakes have been shown to have lower stress drops than tectonic earthquakes (Goertz-Allmann et al., 2011; Hough, 2014).

If there are no further significant earthquakes in the region whilst the local temporary monitoring network is in place, it is possible that we may never be able to resolve in detail the depth and faulting mechanism discrepancies highlighted in this report.

A more robust discrimination of whether the 2018 Surrey earthquakes were natural or induced will require more quantitative analyses of the earthquake characteristics, as well the use of numerical reservoir models to simulate fluid flow and stress transfer, as well as statistical-based models (Grigoli et al., 2017). However, to build such models, more detailed parameters of the local drilling activities will be required, such as higher-resolution (e.g. daily) data of injection and extraction rates and volumes, borehole stress and pressure conditions,

Overall, there is a lack of clear correlation between the 2018 Surrey earthquakes and nearby hydrocarbon activities, and there is some uncertainty over the candidate physical mechanisms that may have induced these earthquakes. Future scientific progress will be needed to better understand the response of sedimentary rocks and basin structures to fluid injection and extraction, even at small volumes and rates. It is possible that with more time and data, such as the long-term continuation of seismic monitoring and detailed data of drilling activities and well parameters to be provided by operators, and with any further changes in seismicity, we may allow us to make a more confident discrimination between natural and induced causes.

[6] http://www.earthquakes.bgs.ac.uk/research/manchester_sequence.html

References

Andrews, I.J., 2014. The Jurassic shales of the Weald Basin: geology and shale oil and shale gas resource estimation.

Assumpção, M., 1981. The NW Scotland earthquake swarm of 1974. Geophys. J. Int. 67, 577–586. doi:10.1111/j.1365-246X.1981.tb06938.x

Baptie, B., 2010. Seismogenesis and state of stress in the UK. Tectonophysics 482, 150–159.

Bent, A.L., Halchuk, S., Peci, V., Butler, K.E., Burke, K.B.S., Adams, J., Dahal, N., Hayek, S., 2017. The McAdam, New Brunswick, Earthquake Swarms of 2012 and 2015–2016: Extremely Shallow, Natural Events. Seismol. Res. Lett. 88, 1586–1600. doi:10.1785/0220170071

Bouchon, M., 1981. A simple method to calculate Green's functions for elastic layered media. B. Seismol. Soc. Am. 71, 959–971.

Butcher, A., Luckett, R., Verdon, J.P., Kendall, J.-M., Baptie, B., Wookey, J., 2017. Local Magnitude Discrepancies for Near-Event Receivers: Implications for the U.K. Traffic-Light Scheme B. Seismol. Soc. Am. 107, 532–541. doi:10.1785/0120160225

Butler, M., Pullan, C.P., 1990. Tertiary structures and hydrocarbon entrapment in the Weald Basin of southern England. Geol. Soc. London Spec. Pub. 55, 371–391. doi:10.1144/GSL.SP.1990.055.01.19

Clarke, H., Eisner, L., Styles, P., Turner, P., 2014. Felt seismicity associated with shale gas hydraulic fracturing: The first documented example in Europe. Geophys. Res. Lett. 41, 8308–8314. doi:10.1002/2014GL062047

Dahm, T., Heimann, S., Funke, S., Wendt, S., Rappsilber, I., Bindi, D., Plenefisch, T., Cotton, F., 2018. Seismicity in the block mountains between Halle and Leipzig, Central Germany: centroid moment tensors, ground motion simulation, and felt intensities of two <Emphasis Type="Italic">M</Emphasis> ≈ 3 earthquakes in 2015 and 2017. J. Seismol. 22, 985–1003. doi:10.1007/s10950-018-9746-9

Davis, S.D., Frohlich, C., 1993. Did (Or Will) Fluid Injection Cause Earthquakes? - Criteria for a Rational Assessment. Seismol. Res. Lett. 64, 207–224.

Dreger, D., Helmberger, D., 1991. Source parameters of the Sierra Madre earthquake from regional and local body waves. Geophys. Res. Lett. doi:10.1029/91GL02366

Dreger, D., Uhrhammer, R., Pasyanos, M., Franck, J., Romanowicz, B., 1998. Regional and far-regional earthquake locations and source parameters using sparse broadband networks: A test on the Ridgecrest sequence. B. Seismol. Soc. Am. 88, 1353–1362. doi:10.1029/93JB00023

Dreger, D.S., Helmberger, D.V., 1993. Determination of source parameters at regional distances with three-component sparse network data. J. Geophys. Res. 98, 8107. doi:10.1029/93JB00023

Ellsworth, W.L., 2013. Injection-Induced Earthquakes. Science 341, 1225942–1225942. doi:10.1126/science.1225942

Fan, G., Wallace, T., 1991. The determination of source parameters for small earthquakes from a single, very broadband seismic station. Geophys. Res. Lett. 18, 1385–1388. doi:10.1029/91GL01804

Frohlich, C., DeShon, H., Stump, B., Hayward, C., Hornbach, M., Walter, J.I., 2016. A Historical Review of Induced Earthquakes in Texas. Seismol. Res. Lett. 87, 1022–1038. doi:10.1785/0220160016

Frohlich, C., Glidewell, J., Brunt, M., 2012. Location and Felt Reports for the 25 April 2010 mbLg 3.9 Earthquake near Alice, Texas: Was it Induced by Petroleum Production?The April 2010 Earthquake near Alice, Texas: Was it Induced by Petroleum Production? B. Seismol. Soc. Am. 102, 457–466. doi:10.1785/0120110179

Gibbons, S.J., Kværna, T., 2017. Illuminating the seismicity pattern of the October 8, 2005, M = 7.6 Kashmir earthquake aftershocks. Phys. Earth. Planet. Inter. 270, 1–8. doi:10.1016/j.pepi.2017.06.008

Goebel, T.H.W., Brodsky, E.E., 2018. The spatial footprint of injection wells in a global compilation of induced earthquake sequences. Science 361, 899–904. doi:10.1126/science.aat5449

Goertz-Allmann, B.P., Goertz, A., Wiemer, S., 2011. Stress drop variations of induced earthquakes at the Basel geothermal site. Geophys. Res. Lett. 38, n/a–n/a. doi:10.1029/2011GL047498

Grigoli, F., Cesca, S., Priolo, E., Rinaldi, A.P., Clinton, J.F., Stabile, T.A., Dost, B., Fernandez, M.G., Wiemer, S., Dahm, T., 2017. Current challenges in monitoring, discrimination, and management of induced seismicity related to underground industrial activities: A European perspective. Rev. Geophys. 55, 310–340.

Holtkamp, S.G., Brudzinski, M.R., 2011. Earthquake swarms in circum-Pacific subduction zones. Earth Planet. Sci. Lett. 305, 215–225.

Hough, S.E., 2014. Shaking from Injection-Induced Earthquakes in the Central and Eastern United StatesShort Note. B. Seismol. Soc. Am. 104, 2619–2626. doi:10.1785/0120140099

Kusznir, N.J., Ashwin, D.P., Bradley, A.G., 1980. Mining induced seismicity in the North Staffordshire coalfield, England. International Journal of Rock Mechanics and Mining Sciences & Geomechanics Abstracts 17, 45–55.

Laske, G., Masters, G., Ma, Z., Pasyanos, M., 2013. Update on CRUST1. 0—A 1-degree global model of Earth's crust, in:. Presented at the Geophys. Res. Abstr, EGU General Assembly Vienna, Austria, p. 2658.

Lomax, A., Michelini, A., Curtis, A., 2009. Earthquake location, Direct, Global-search Methods, in: Meyers, R.A. (Ed.), Encyclopedia of Complexity and Systems Science, Encyclopedia of Complexity and Systems Science. Springer New York, New York, NY, pp. 2449–2473. doi:10.1007/978-0-387-30440-3_150

Myers, S.C., Johannesson, G., Hanley, W., 2007. A Bayesian hierarchical method for multiple-event seismic location. Geophys. J. Int. 171, 1049–1063. doi:10.1111/j.1365-246X.2007.03555.x

Ottemöller, L., Nielsen, H.H., Atakan, K., Braunmiller, J., Havskov, J., 2005. The 7 May 2001 induced seismic event in the Ekofisk oil field, North Sea. J. Geophys. Res. 110, 379. doi:10.1029/2004JB003374

Ottemöller, L., Sargeant, S., 2013. A Local Magnitude Scale ML for the United Kingdom. B. Seismol. Soc. Am. 103, 2884–2893. doi:10.1785/0120130085

Ottemöller, L., Thomas, C.W., 2007. Highland Boundary Fault Zone: Tectonic implications of the Aberfoyle earthquake sequence of 2003. Tectonophysics 430, 83–95.

Ristau, J., 2008. Implementation of Routine Regional Moment Tensor Analysis in New Zealand. Seismol. Res. Lett. 79, 400–415. doi:10.1785/gssrl.79.3.400

Simpson, D.W., Leith, W.S., Scholz, C.H., 1988. Two types of reservoir-induced seismicity. B. Seismol. Soc. Am. 78, 2025–2040.

Skoumal, R.J., Brudzinski, M.R., Currie, B.S., 2015. Distinguishing induced seismicity from natural seismicity in Ohio: Demonstrating the utility of waveform template matching. J. Geophys. Res. Solid Earth 120, 6284–6296. doi:10.1002/2015JB012265

Sokos, E.N., Zahradnik, J., 2006. A Matlab GUI for use with ISOLA Fortran codes. Users' guide.

Vidale, J.E., Shearer, P.M., 2006. A survey of 71 earthquake bursts across southern California: Exploring the role of pore fluid pressure fluctuations and aseismic slip as drivers. J. Geophys. Res. 111, n/a–n/a. doi:10.1029/2005JB004034

Wang, R., 1999. A simple orthonormalization method for stable and efficient computation of Green's functions. B. Seismol. Soc. Am. 89, 733–741.

Wilson, M.P., Davies, R.J., Foulger, G.R., Julian, B.R., Styles, P., Gluyas, J.G., Almond, S., 2015. Anthropogenic earthquakes in the UK: A national baseline prior to shale exploitation. Marine and Petroleum Geology 68, 1–17. doi:10.1016/j.marpetgeo.2015.08.023